# Differentiating and Quantifying Gas-Phase Conformational Isomers using Coulomb Explosion Imaging

Shashank Pathak[1,*], Razib Obaid[2,#], Surjendu Bhattacharyya[1], Johannes Bürger[3], Xiang Li[1], Jan Tross[1,##], Travis Severt[1], Brandin Davis[2], René C. Bilodeau[2,4], Carlos Trallero[2], Artem Rudenko[1], Nora Berrah[2] and Daniel Rolles[1,*]

[1]*J.R. Macdonald Laboratory, Department of Physics, Kansas State University, Manhattan, KS, USA*
[2]*Department of Physics, University of Connecticut, Storrs, CT, USA*
[3]*Department of Physics, Ludwig Maximilian University of Munich, Germany*
[4]*Advanced Light Source, Lawrence Berkeley National Laboratory, Berkeley, CA*
[#]*Current address - RARAF, Columbia University, Irvington, NY, USA.*
[##]*Current address – Sandia National Lab*
*Corresponding author - *rolles@phys.ksu.edu, *shashankp@phys.ksu.edu*

## Abstract

Conformational isomerism plays a crucial role in defining the physical and chemical properties and biological activity of molecules ranging from simple organic compounds to complex biopolymers. However, it is often a significant challenge to differentiate and separate these isomers experimentally as they can easily interconvert due to their low rotational energy barrier. Here, we use the momentum correlation of fragment ions produced after inner-shell photoionization to distinguish conformational isomers of 1,2-dibromoethane ($C_2H_4Br_2$). We demonstrate that the three-body breakup channel, $C_2H_4^+ + Br^+ + Br^+$, contains signatures of both sequential and concerted breakup, which are decoupled to distinguish the geometries of two conformational isomers and to quantify their relative abundance. The sensitivity of our method to quantify these yields is established by measuring the relative abundance change with sample temperature, which agrees well with calculations. Our study paves the way for using Coulomb explosion imaging to track subtle molecular structural changes.

## TOC

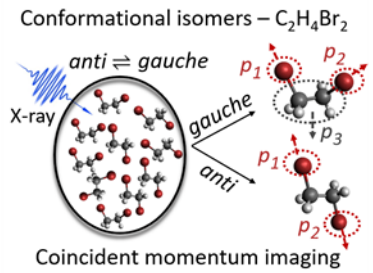


**Keywords** Photochemistry, Conformational Isomerism, Momentum Imaging, Native-Frames, Photoionization

Conformational isomers, or conformers, are defined as molecules with the same chemical formula but different geometrical structures, caused by rotation around a single bond[1]. Conformational isomerism is a common phenomenon in a wide range of molecules from simple polyatomics to large biomolecules and plays a crucial role, e.g., in their biological activity and molecular recognition[2]. Several neurological diseases are known to be caused by altered protein conformations[3]. Consequently, conformational isomerism is omnipresent in the present-day pharmaceutical industry, and it closely defines the activity of drug molecules[4]. Conformations also dictate physical and chemical properties, including photoabsorption. However, studying conformer-specific properties, even for small molecules, represents a major experimental challenge since they can interconvert. This internal rotation of one conformer into another is extremely prevalent even at room temperature because of the low rotational energy barrier between different conformers, which is usually a few kcal/mol.

Due to its ubiquity and fundamental nature, conformational isomerism continues to be investigated in a variety of systems using different experimental methods. In recent years, several investigations have studied conformer-specific photodissociation[5-6] and photoinduced conformations[7] for unimolecular reactions. Some of these studies have not only shown strong conformation specific reaction yields but have also uncovered disagreement with predictions from statistical rate theory[8], which warrants further investigations on different systems. Gas-phase studies of conformational isomers would strongly benefit from techniques that are able to separate or distinguish isomers in dilute molecular beams. One such method spatially separates the conformers in a molecular beam by deflecting them in an inhomogeneous electric field[9], thus exploiting the difference in inherent dipole moments of the isomers. However, this method has difficulties in separating non-polar molecules. Recently, the mega electron-volt ultrafast electron diffraction (MeV-UED) technique was used to distinguish transient conformational structures of photoexcited 1,2-diiodotetrafluoroethane molecules.[10]

Another simple yet powerful technique for structure determination in single molecules is Coulomb explosion imaging[11] (CEI) in a coincident ion momentum imaging mode[12-13]. Photon-induced CEI has been demonstrated using different light sources including femtosecond lasers[14-19], synchrotron radiation sources[20-21], and free-electron lasers[22] in recent years. Here, we show that CEI using coincident ion momentum imaging is a suitable method to differentiate and quantify conformational isomers and to study conformer specific photoabsorption properties. Our experiment is performed on 1,2-dibromoethane ($C_2H_4Br_2$), also known as ethylene dibromide (EDB). EDB is a simple organobromide that is often scrutinized due to its environmental impact[23], which makes it a pressing target for light-induced studies. EDB is known to exist in both the *anti* and *gauche* conformations, which are separated in this study using coincident ion momentum imaging in combination with state-of-the-art analysis techniques that allow structure determination on a molecule-by-molecule level. Specifically, we consider the three-body fragmentation of EDB after bromine 3*d* inner-shell ionization at 140 eV photon energy (see Methods) and use the momenta of three ionic fragments detected in coincidence to determine the geometry of EDB prior to fragmentation. The kinetic energies and the angular correlation between the ionic fragments give a clear signature of two different geometries, which are assigned to *gauche* and *anti* conformers of EDB based on classical Coulomb explosion simulations. To test the sensitivity of our method, we analyze the change in the ratio of the measured yield of these conformers with the

change in temperature of the sample. The results of the experiment performed at three different temperatures agree well with the theoretically expected change in the ratio of *gauche* to *anti* conformers in the molecular beam.

The molecular structure of the *gauche* and *anti* conformers of EDB are shown in Figure 1(a). The interconversion happens by the rotation around C-C bond. Figure 1(b) shows a region of the triple ion coincidence spectrum near the channel of interest for this study, $C_2H_4^+ + Br^+ + Br^+$. The time-of-flight of the first detected light fragment ion (TOF1) is shown on the x-axis, the sum of the times of flight of the second and third heavier fragment ions (TOF2+TOF3) on the y-axis, while the color represents the yield of the corresponding triple coincidence events. For breakup channels where no further fragments with significant momentum are produced, the triple-ion-coincidence plot shows sharp diagonal lines due to momentum conservation during the breakup process.

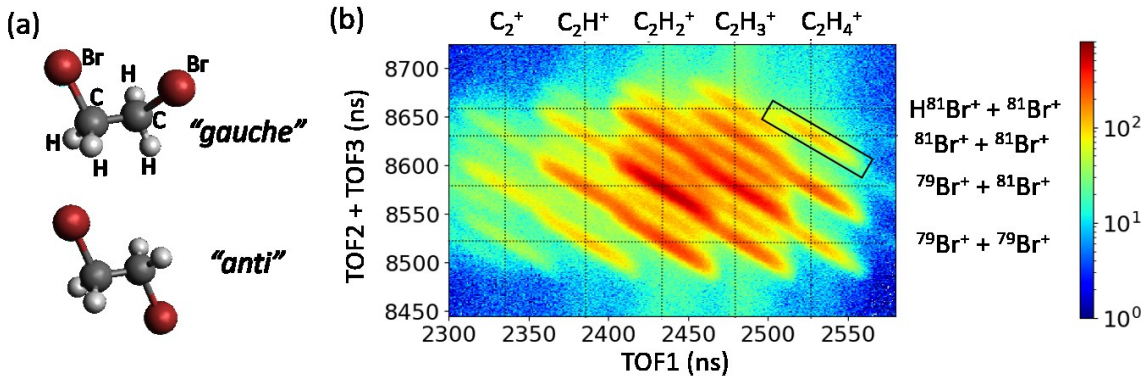


**Figure 1.** (a) *Gauche* and *anti* conformations of 1,2 dibromoethane (EDB, $C_2H_4Br_2$). (b) Triple-ion coincident time-of-flight spectrum for EDB zoomed in near the channel of interest (marked by the black rectangle).

Each diagonal line corresponds to a specific three-body fragmentation channel, whose relative yields are given in the Supporting Information. For the present investigation, we focus on the $C_2H_4^+ + {}^{81}Br^+ + {}^{81}Br^+$ coincidence channel as it is well separated from other channels and gives a clear indication of the geometry before fragmentation, as explained in the following. The momenta and kinetic energies of the three coincident ions are calculated from the time of flight and detector hit position of each ion (see Supporting Information, Section 1), and the results are shown in Figure 2(a) as a Newton plot, which allows an intuitive visualization of the momentum correlations[24]. Here, the momentum of one of the ${}^{81}Br^+$ ion is fixed to unity, and the normalized relative momenta (magnitude and direction) of $C_2H_4^+$ and the other ${}^{81}Br^+$ are plotted in the upper ($y>0$) and lower ($y<0$) half of the plot, respectively. For the selected breakup channel, the Newton plot shows two semi-circular structures and several local maxima (yellow spots) that partially overlap with the semi-circles. These features need to be understood and deconvoluted to separate the contribution from *gauche* and *anti* conformers. Semi-circular structures in a Newton plot are typically a consequence of a *sequential* breakup[25], while the local maxima are due to *concerted (synchronous)* breakup of EDB subsequent to photoionization. Equation (1) and (2) show examples of concerted and sequential breakup pathways that contribute to the selected coincidence channel:

$C_2H_4Br_2^{3+}$ → $C_2H_4^+ + Br^+ + Br^+$ (*concerted / synchronous*) (1)

$C_2H_4Br_2^{3+}$ → $C_2H_4Br^{2+} + Br^+$ → $C_2H_4^+ + Br^+ + Br^+$ (*sequential*) (2)

The breakage of two molecular bonds in a tri-cation is defined as *sequential* if an intermediate di-cation (here: $C_2H_4Br^{2+}$) is formed with a lifetime longer than its rotational period[26]. The semi-circular ring in the Newton plot is thus a manifestation of the rotation of the intermediate di-cation.

Figure 2(b) shows the kinetic energy distribution of individual fragment ions and the kinetic energy release (KER). The rather broad distribution in kinetic energies of the fragments also suggests the presence of several contributing channels, such as both concerted and sequential fragmentation, as well as the presence of *gauche* and *anti* conformers. Only the concerted breakup pathways can be used to extract the molecular geometry using CEI[27], hence the sequential pathways need to first be disentangled by further analysis.

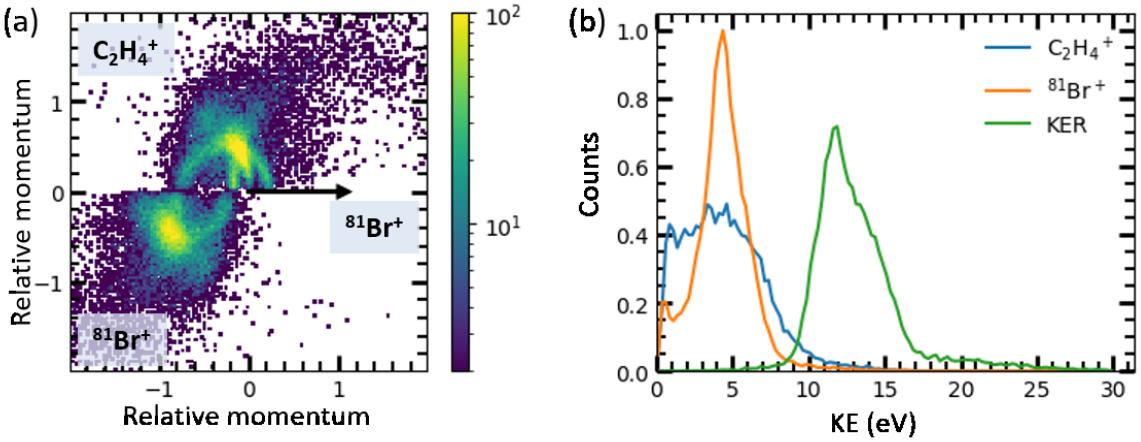


**Figure 2.** Newton plot (a) and kinetic energy distributions (b) of $C_2H_4^+$ (blue) and $^{81}Br^+$ (orange) fragments and sum of the three ion kinetic energies or KER (green) for the $C_2H_4^+ + {}^{81}Br^+ + {}^{81}Br^+$ coincidence channel. The Newton plot shows the normalized relative momenta of $C_2H_4^+$ and $^{81}Br^+$ plotted with respect to the other $^{81}Br^+$ (represented by the black arrow), whose momentum is fixed to unity in the positive X-direction.

For separating the concerted breakup events from the sequential breakup events, we use the recently developed *native frames* method[28]. To briefly summarize, the native frames method takes advantage of the rotation of the intermediate metastable molecular fragment produced during a sequential breakup to distinguish sequential from concerted fragmentation. The main idea of the native frames method is to analyze each fragmentation step in its respective center-of-mass reference frame, i.e. its *native* frame, which we accomplish using the conjugate momenta derived from Jacobi coordinates associated with each fragmentation step (see Supporting Information, Figure S3). Then, we identify sequential fragmentation as a uniform angular distribution between the conjugate momenta for each step, assuming that the intermediate fragment (di-cation) is rotating in the fragmentation plane. By taking advantage of the uniform angular distribution, we reconstruct parts of the distribution of sequential breakup events masked by competing concerted fragmentation, allowing us to separate the sequential and concerted breakup distributions in any

plot created from the measured momenta. More details regarding the application of the native frames analysis on EDB can be found in the Supporting Information.

As the first step in the native frames method, Figure 3(a) shows all three-body fragmentation events in the $C_2H_4^+ + {}^{81}Br^+ + {}^{81}Br^+$ breakup channel, plotted as a function of the second-step kinetic energy release, $KER_{C_2H_4 81_{Br}}$, and the angle between the relative momenta describing each step of sequential fragmentation with $(C_2H_4{}^{81}Br)^{2+}$ as intermediate di-cation, $\theta_{C_2H_4 81_{Br},\, 81_{Br}}$. The second-step KER is obtained using the relative momentum of the second step[28]. In this representation, the events in the vertical structure at $KER_{C_2H_4 81_{Br}} \approx 4\ eV$ (shown by black arrow), which are uniformly distributed over all angles, stem from sequential fragmentation. For the further analysis, they can be subtracted, as detailed in the Supporting Information, such that all following plots contain only coincidence events from a concerted breakup.

In order to identify and separate the contributions corresponding to concerted breakup of *gauche* and *anti* conformers, which are partially overlapping in the Newton plot (see Supporting Information, Figure S5). Figure 3(b) shows a plot similar to Figure 3(a), but after subtraction of the sequential events and choosing a hypothetical $({}^{81}Br\ {}^{81}Br)^{2+}$ intermediate di-cation for the representation. In other words, the relative momenta used in Figure 3(b) are calculated for a hypothetical sequential breakup with a $({}^{81}Br\ {}^{81}Br)^{2+}$ intermediate (see Supporting Information). We can clearly identify two different contributions and select each contribution by gating on the regions of interest (ROI) shown by the black rectangles. To verify this selection, the fragment kinetic energies for the events selected in each of the two ROIs in Figure 3(b) are plotted in Figure 3(c) and 3(d), which show two distinctly different patterns. From Figure 3(c), it is apparent that for the *gauche* conformer, the $C_2H_4^+$ fragment is produced with higher kinetic energy as compared to the ${}^{81}Br^+$ fragments since it is repelled by both ${}^{81}Br^+$ fragments, which are emitted in the same hemisphere. For the *anti* conformer (Figure 3(d)), the kinetic energy of the $C_2H_4^+$ fragment is smaller than that of the ${}^{81}Br^+$ fragments since the $C_2H_4^+$ fragment is trapped in between the two ${}^{81}Br^+$ fragments as they impart their momenta onto the $C_2H_4^+$ fragment in almost exactly opposite directions, a condition often referred to as 'obstructed instantaneous explosion'[29].

The dashed lines in Figure 3(c) and 3(d) show the results of a Coulomb explosion simulation (CES) performed for concerted breakup of both conformers. The simulation starts from the equilibrium geometry of the neutral conformers and assumes point charges at the positions of two bromine atoms and at the center-of-mass (c.o.m.) of the third fragment ($C_2H_4$). For each point charge, a small random variation of the position within a sphere corresponding to a 5% change in one of the C-Br bond-lengths is chosen in order to account for small geometry changes of the molecule prior to fragmentation, e.g., as a result of vibrations in the neutral or ionic states, either due to the initial temperature of the sample or due to vibrational excitation during the ionization process. The trajectories (and hence velocities and momenta) for 1000 such "near-equilibrium" geometries for both conformations are calculated by numerically solving the classical equations of motions assuming pure Coulombic repulsive interaction between the point charges (see Supporting Information, section 3). The simulation results reproduce the overall observations in the experimental data but overestimate the energies for each fragment. Such overestimation of the kinetic energies is common for simple CES and can indicate an increase of the bond lengths prior

to fragmentation; tri-cationic potential energy surfaces that are not purely Coulombic; or a finite internal energy stored in the fragments[30].

Figure 4(a) and 4(c) show the Newton plots for the *gauche* and *anti* conformers in the experiment, separated as described above, while Figure 4(b) and 4(d) show the simulated Newton plots obtained from the CES. The good agreement between simulation and experimental results further confirms that the separated events indeed correspond to the concerted breakup events from different conformers. Therefore, the ratio of *gauche* to *anti* conformers can simply be determined from the respective yields in the ROIs in Fig. 3(b), and we can, in the following, investigate the change in the conformer ratio as a function of sample temperature.

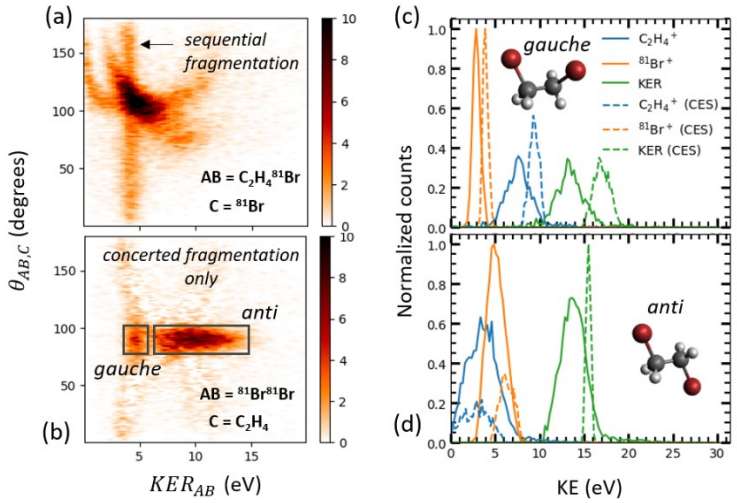


**Figure 3.** (a) All events in the $C_2H_4^+ + {}^{81}Br^+ + {}^{81}Br^+$ coincidence channel, plotted as a function of second-step KER ($KER_{C_2H_4 81_{Br}}$) and angle ($\theta_{C_2H_4 81_{Br}, 81_{Br}}$) between the relative momenta describing each step of a sequential fragmentation with $(C_2H_4{}^{81}Br)^{2+}$ as the intermediate di-cation (see text). (b) Similar to panel (a), but after subtraction of sequential breakup events using the native frames method and plotted for a hypothetical intermediate di-cation $({}^{81}Br{}^{81}Br)^{2+}$. The black rectangles show the ROIs chosen to separate *anti* and *gauche* conformers. (c), (d) Experimental kinetic energy distributions (solid lines) for the fragments and total KER for *gauche* and *anti* conformers selected from panel (b) along with results from Coulomb explosion simulations (CES, dashed lines) for both cases.

Conformational isomers often coexist in a dynamic equilibrium, with the conformer ratio being determined by temperature of the system and the difference in free energies of the conformers. This can be expressed as[31]:

$$\Delta G = -RT \ln(K), \qquad (3)$$

where $\Delta G$ is the difference in the free energy of the two conformers, R is the universal gas constant, T is the temperature of the sample, and K is the equilibrium constant, which, in the present case, corresponds to the ratio of *gauche* and *anti* conformers. In order to verify the ability of our CEI technique to quantify the conformer ratio and to test its sensitivity, we recorded fragmentation data for EDB at three different sample temperatures while keeping all other experimental parameters constant. The three different temperatures, measured at the molecular beam nozzle, were $T_1 = 20^{\circ}C$

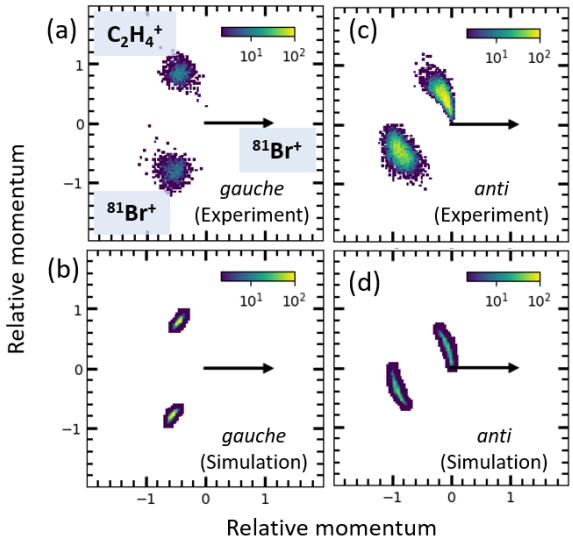


**Figure 4.** (a), (b) Newton plots from experimental data and CES for *gauche* conformer. (c), (d) Newton plots from experimental data and CES for *anti* conformer.

(i.e. without heating), $T_2$ = 60˚C, and $T_3$ = 95˚C. The theoretical estimate of the *gauche* to *anti* ratio for EDB can be calculated using eq. (3). For the equilibrium, *anti* ⇌ *gauche*, the degrees of freedom are the same between the reactant and product. We thus assume $\Delta S = 0$, which implies $\Delta G = \Delta H$, where $\Delta H$ is the change in enthalpy and $\Delta S$ is the change in entropy. To determine the energy barrier and enthalpy difference between the *gauche* and *anti* conformers, quantum chemical calculations were performed using the Gaussian software package[32] (see Methods). These values were then used to calculate the expected ratio of *gauche* to *anti* conformer for different temperatures using eq. (3). Here, our assumption is that the vibrational degrees of freedom do not cool significantly during the expansion in the molecular beam nozzle, which is generally true for small molecules[33] but, to the best of our knowledge, has not been studied for complex molecules such as dibromoethane. This allows us to consider the sample temperature to be equal to the nozzle temperature.

Figure 5(a) shows the coincident ion yield of the experiment attributed to *gauche* and *anti* conformers for the three temperatures. The yield of the *gauche* conformer clearly increases at higher temperatures while the yield of the *anti* conformer decreases. This is expected since more molecules can cross the rotational energy barrier between *anti* and *gauche* conformers at higher temperatures. Figure 5(b) shows the resulting *gauche* to *anti* ratio obtained from the experiment compared to the theoretical values (shown in blue) obtained using eq. (3). The error bars on the experimental data show the statistical error. The blue band around the theoretical curve shows the variation in the theoretical value corresponding to an uncertainty of the absolute temperature of +/- 10˚C in order to visualize the uncertainty in the ratio, e.g., due to possible differences between the thermocouple readings and the actual temperature of the sample. The experimental and theoretical values are in good agreement except at room temperature, where the experiment yields a larger amount of *gauche* conformer than predicted by theory. We attribute this to the very small

contribution (in absolute numbers) of *gauche* conformers at room temperature, which makes the value for the ion yield from *gauche* conformers more susceptible to small contributions from "background" counts that may not be fully discriminated (see Figure 3(b) and Supporting Information - Figure S4b, S4c). Furthermore, we note that the overall good agreement between experiment and theory suggests that the triple ionization and dissociation probability into the channel of interest is the same for each conformer, which is reasonable for inner-shell ionization but may be different, e.g., for strong-field ionization.

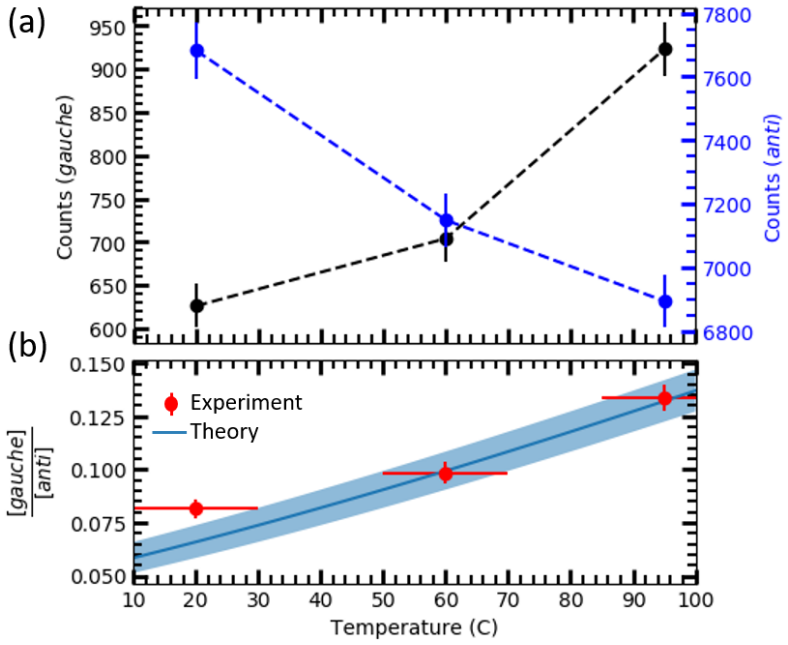


**Figure 5.** (a) Experimental yield of *gauche* (black) and *anti* (blue) conformer as a function of sample temperature. The yield of *gauche* conformer increases and *anti* conformer decreases, suggesting an increased conversion from *anti* to *gauche* at higher temperature, as expected based on the difference in the free energy of the two conformers. (b) Theoretical and experimental change in ratio as a function of sample temperature. The blue band represents the uncertainty of the theoretical ratio when assuming an uncertainty of +/- 10˚C in the sample temperature.

In conclusion, we have demonstrated that we can distinguish and quantify the yields of the conformational isomers of EDB, which co-exist in a dynamic equilibrium and are separated by an extremely small energy difference (~1/10 eV). Specifically, our methodology can distinguish between *anti* and *gauche* conformers of EDB by selecting triple ion coincidences combined with a detailed analysis of the different fragmentation pathways using Newton plots and fragment kinetic energies combined with the novel native frames analysis technique. Our measurements performed at different sample temperatures indicate that our technique is sensitive to subtle change in the conformer ratio and in good agreement with theoretical calculations. This level of sensitivity

of CEI technique is crucial for future molecular dynamics studies, such as time-resolved experiments studying the interconversion of conformers, where the quantitative determination of small changes in conformer population is essential.

## Methods

The experiment was performed at beamline 10.0.1.3 of the Advanced Light Source (ALS) at the Lawrence Berkeley National Laboratory. Fragment ions and electrons were measured in coincidence using a double-sided velocity map imaging (VMI) spectrometer. The VMI spectrometer and data collection has been described elsewhere in detail[34]. EDB was introduced into the ultra-high vacuum experimental chamber, using a supersonic expansion through a nozzle of 30 μm in diameter. The molecular beam is skimmed by using a 500 μm skimmer before it interacts with the soft X-ray photons at the interaction region inside the VMI spectrometer. The experiment was performed at a photon energy of 140 eV (bandwidth: 15 meV), which is above the 3*d* photoionization threshold (~77.5 eV) of Br and near the (broad) peak of the 3*d* giant resonance found in Br-containing molecules[35]. As the resonantly enhanced Br 3*d* photoionization cross section dominates the total cross section at this photon energy, photoionization occurs predominantly by removal of a 3*d* inner-shell electron, followed by an Auger process that emits one or two further electrons. As the multiply charged EDB molecule dissociates into fragment ion, the time-of-flight and position of all the ionic fragments are recorded, which are then used to calculate the three-dimensional momenta and kinetic energies for each ion recorded in coincidence[34].

Quantum chemical calculations were performed for calculating the enthalpy difference between the conformers. Both conformer structures were initially optimized at the ωB97X-D level of theory[36] using the 6-31G basis set to estimate the electronic energies. The energies were verified against different choices of basis sets. The highest methodology used was MP2, and the largest basis set used was aug-cc-pVDZ, which gave an enthalpy difference between the *gauche* and *anti* conformers of $\Delta H$ = 0.086 eV (1.985 kcal/mol), after zero-point energy correction. Our calculations also match with previous work[37] where the computations were performed at MP2/6-311++G(d, p) level of theory and yielded a value of 0.091 eV (2.099 kcal/mol). These values are approximately 15% higher than the experimentally determined value of 1.68 kcal/mol found by infrared absorption measurements performed in a gas cell[38]. We note that the *gauche* conformer exists as *gauche*$^+$ and *gauche*$^-$, which are mirror images of one another and have the same enthalpy. For the theoretical calculation, they are considered as two separate dynamic equilibria with the *anti* conformer. Since the CEI technique cannot distinguish between *gauche*$^+$ and *gauche*$^-$, we therefore multiply the theoretically calculated *gauche* to *anti* ratio by a factor of 2 to account for the two types of *gauche* conformer.

## Associated content

**Supporting Information:** Experimental details and momentum reconstruction, Subtraction of sequential events using native frames method and Coulomb explosion simulation (CES) for the concerted breakup channel $C_2H_4^+ + Br^+ + Br^+$

## Author Information

**Notes –** The authors declare no competing financial interest.

## Acknowledgements

This work is supported by the U.S, Geosciences, and Biosciences Division, Office of Basic Energy Sciences, Office of Science, US Department of Energy, grant no. DE-FG02-86ER13491 (Kansas group) and DE-SC0012376 (UConn group). S.B was supported by grant no. DE-SC0020276 from the same funding agency, and J.T. was supported by the National Science Foundation (NSF) grant PHYS-1753324. J.B. acknowledges support through the DAAD RISE program. This research used resources of the Advanced Light Source, which is a DOE Office of Science User Facility under contract no. DE-AC02-05CH11231. We thank the staff of the Advanced Light Source for their hospitality and their help during the beamtime.

## References

1. *IUPAC. Compendium of Chemical Terminology, 2nd ed. (the "Gold Book")*. 1994.

2. Boehr, D. D.; Nussinov, R.; Wright, P. E. The role of dynamic conformational ensembles in biomolecular recognition. *Nature Chemical Biology* **2009,** *5* (11), 789-796.

3. Sweeney, P.; Park, H.; Baumann, M.; Dunlop, J.; Frydman, J.; Kopito, R.; McCampbell, A.; Leblanc, G.; Venkateswaran, A.; Nurmi, A.; Hodgson, R. Protein misfolding in neurodegenerative diseases: implications and strategies. *Transl Neurodegener* **2017,** *6*, 6-6.

4. Harrold, M. W. The Influence of Conformational Isomerism on Drug Action and Design *American Journal of Pharmaceutical Education* **1996,** *60*, 192-197.

5. Kim, M. H.; Shen, L.; Tao, H.; Martinez, T. J.; Suits, A. G. Conformationally Controlled Chemistry: Excited-State Dynamics Dictate Ground-State Reaction. *Science* **2007,** *315* (5818), 1561.

6. Park, S. T.; Kim, S. K.; Kim, M. S. Observation of conformation-specific pathways in the photodissociation of 1-iodopropane ions. *Nature* **2002,** *415* (6869), 306-308.

7. Dian, B. C.; Clarkson, J. R.; Zwier, T. S. Direct Measurement of Energy Thresholds to Conformational Isomerization in Tryptamine. *Science* **2004,** *303* (5661), 1169.

8. Dian, B. C.; Brown, G. G.; Douglass, K. O.; Pate, B. H. Measuring Picosecond Isomerization Kinetics via Broadband Microwave Spectroscopy. *Science* **2008,** *320* (5878), 924.

9. Chang, Y.-P.; Długołęcki, K.; Küpper, J.; Rösch, D.; Wild, D.; Willitsch, S. Specific Chemical Reactivities of Spatially Separated 3-Aminophenol Conformers with Cold Ca<sup>+</sup> Ions. *Science* **2013,** *342* (6154), 98.

10. Wilkin, K. J.; Parrish, R. M.; Yang, J.; Wolf, T. J. A.; Nunes, J. P. F.; Guehr, M.; Li, R.; Shen, X.; Zheng, Q.; Wang, X.; Martinez, T. J.; Centurion, M. Diffractive imaging of dissociation and ground-state dynamics in a complex molecule. *Physical Review A* **2019,** *100* (2), 023402.

11. Vager, Z.; Naaman, R.; Kanter, E. P. Coulomb Explosion Imaging of Small Molecules. *Science* **1989,** *244* (4903), 426.

12. Pitzer, M.; Kunitski, M.; Johnson, A. S.; Jahnke, T.; Sann, H.; Sturm, F.; Schmidt, L. P. H.; Schmidt-Böcking, H.; Dörner, R.; Stohner, J.; Kiedrowski, J.; Reggelin, M.; Marquardt, S.; Schießer, A.; Berger, R.; Schöffler, M. S. Direct Determination of Absolute Molecular Stereochemistry in Gas Phase by Coulomb Explosion Imaging. *Science* **2013,** *341* (6150), 1096.

13. Pitzer, M.; Kastirke, G.; Kunitski, M.; Jahnke, T.; Bauer, T.; Goihl, C.; Trinter, F.; Schober, C.; Henrichs, K.; Becht, J.; Zeller, S.; Gassert, H.; Waitz, M.; Kuhlins, A.; Sann, H.; Sturm, F.; Wiegandt, F.; Wallauer, R.; Schmidt, L. P. H.; Johnson, A. S.; Mazenauer, M.; Spenger, B.; Marquardt, S.; Marquardt, S.; Schmidt-Böcking, H.; Stohner, J.; Dörner, R.; Schöffler, M.; Berger, R. Absolute Configuration from Different Multifragmentation Pathways in Light-Induced Coulomb Explosion Imaging. *ChemPhysChem* **2016,** *17* (16), 2465-2472.

14. Hishikawa, A.; Matsuda, A.; Fushitani, M.; Takahashi, E. J. Visualizing Recurrently Migrating Hydrogen in Acetylene Dication by Intense Ultrashort Laser Pulses. *Physical Review Letters* **2007,** *99* (25), 258302.

15. Christensen, L.; Nielsen, J. H.; Brandt, C. B.; Madsen, C. B.; Madsen, L. B.; Slater, C. S.; Lauer, A.; Brouard, M.; Johansson, M. P.; Shepperson, B.; Stapelfeldt, H. Dynamic Stark Control of Torsional Motion by a Pair of Laser Pulses. *Physical Review Letters* **2014,** *113* (7), 073005.

16. Ibrahim, H.; Wales, B.; Beaulieu, S.; Schmidt, B. E.; Thiré, N.; Fowe, E. P.; Bisson, É.; Hebeisen, C. T.; Wanie, V.; Giguére, M.; Kieffer, J.-C.; Spanner, M.; Bandrauk, A. D.; Sanderson, J.; Schuurman, M. S.; Légaré, F. Tabletop imaging of structural evolutions in chemical reactions demonstrated for the acetylene cation. *Nature Communications* **2014,** *5* (1), 4422.

17. Burt, M.; Amini, K.; Lee, J. W. L.; Christiansen, L.; Johansen, R. R.; Kobayashi, Y.; Pickering, J. D.; Vallance, C.; Brouard, M.; Stapelfeldt, H. Communication: Gas-phase structural isomer identification by Coulomb explosion of aligned molecules. *The Journal of Chemical Physics* **2018,** *148* (9), 091102.

18. Kling, N. G.; Díaz-Tendero, S.; Obaid, R.; Disla, M. R.; Xiong, H.; Sundberg, M.; Khosravi, S. D.; Davino, M.; Drach, P.; Carroll, A. M.; Osipov, T.; Martín, F.; Berrah, N. Time-resolved molecular dynamics of single and double hydrogen migration in ethanol. *Nature Communications* **2019,** *10* (1), 2813.

19. McDonnell, M.; LaForge, A. C.; Reino-González, J.; Disla, M.; Kling, N. G.; Mishra, D.; Obaid, R.; Sundberg, M.; Svoboda, V.; Díaz-Tendero, S.; Martín, F.; Berrah, N. Ultrafast Laser-Induced Isomerization Dynamics in Acetonitrile. *The Journal of Physical Chemistry Letters* **2020,** *11* (16), 6724-6729.

20. Ablikim, U.; Bomme, C.; Xiong, H.; Savelyev, E.; Obaid, R.; Kaderiya, B.; Augustin, S.; Schnorr, K.; Dumitriu, I.; Osipov, T.; Bilodeau, R.; Kilcoyne, D.; Kumarappan, V.; Rudenko, A.; Berrah, N.; Rolles, D. Identification of absolute geometries of cis and trans molecular isomers by Coulomb Explosion Imaging. *Scientific Reports* **2016,** *6* (1), 38202.

21. Ablikim, U.; Bomme, C.; Savelyev, E.; Xiong, H.; Kushawaha, R.; Boll, R.; Amini, K.; Osipov, T.; Kilcoyne, D.; Rudenko, A.; Berrah, N.; Rolles, D. Isomer-dependent fragmentation dynamics of inner-shell photoionized difluoroiodobenzene. *Physical Chemistry Chemical Physics* **2017,** *19* (21), 13419-13431.

22. Liekhus-Schmaltz, C. E.; Tenney, I.; Osipov, T.; Sanchez-Gonzalez, A.; Berrah, N.; Boll, R.; Bomme, C.; Bostedt, C.; Bozek, J. D.; Carron, S.; Coffee, R.; Devin, J.; Erk, B.; Ferguson, K. R.; Field, R. W.; Foucar, L.; Frasinski, L. J.; Glownia, J. M.; Gühr, M.; Kamalov, A.; Krzywinski, J.; Li, H.; Marangos, J. P.; Martinez, T. J.; McFarland, B. K.; Miyabe, S.; Murphy, B.; Natan, A.; Rolles, D.; Rudenko, A.; Siano, M.; Simpson, E. R.; Spector, L.; Swiggers, M.; Walke, D.; Wang, S.; Weber, T.; Bucksbaum, P. H.; Petrovic, V. S. Ultrafast isomerization initiated by X-ray core ionization. *Nature Communications* **2015,** *6* (1), 8199.

23. Christiansen, C. J.; Francisco, J. S. Atmospheric Oxidation Mechanism of 1,2-Dibromoethane. *The Journal of Physical Chemistry A* **2009,** *113* (26), 7189-7204.

24. Hsieh, S.; Eland, J. H. D. Reaction dynamics of three-body dissociations in triatomic molecules from single-photon double ionization studied by a time- and position-sensitive coincidence method. *Journal of Physics B Atomic Molecular Physics* **1997,** *30*, 4515-4534.

25. Neumann, N.; Hant, D.; Schmidt, L. P. H.; Titze, J.; Jahnke, T.; Czasch, A.; Schöffler, M. S.; Kreidi, K.; Jagutzki, O.; Schmidt-Böcking, H.; Dörner, R. Fragmentation Dynamics of ${\mathrm{CO}}_{2}^{3+}$ Investigated by Multiple Electron Capture in Collisions with Slow Highly Charged Ions. *Physical Review Letters* **2010,** *104* (10), 103201.

26. Maul, C.; Gericke, K.-H. Photo induced three body decay. *International Reviews in Physical Chemistry* **1997,** *16* (1), 1-79.

27. Hu, X.; Peng, Y.; Zhu, X.; Yan, S.; Liu, L.; Feng, W.; Guo, D.; Gao, Y.; Zhang, S.; Zhao, D.; Dong, D.; Hai, B.; Xu, J.; Zhang, S.; Ma, X.; Wang, J.; Wu, Y. Breakdown of the Coulomb-explosion imaging technique induced by the ultrafast rotation of fragments. *Physical Review A* **2020,** *101* (1), 012707.

28. Rajput, J.; Severt, T.; Berry, B.; Jochim, B.; Feizollah, P.; Kaderiya, B.; Zohrabi, M.; Ablikim, U.; Ziaee, F.; Raju P, K.; Rolles, D.; Rudenko, A.; Carnes, K. D.; Esry, B. D.; Ben-Itzhak, I. Native Frames: Disentangling Sequential from Concerted Three-Body Fragmentation. *Physical Review Letters* **2018,** *120* (10), 103001.

29. Eland, J. H. D. The dynamics of three-body dissociations of dications studied by the triple coincidence technique PEPIPICO. *Molecular Physics* **1987,** *61* (3), 725-745.

30. Légaré, F.; Lee, K. F.; Litvinyuk, I. V.; Dooley, P. W.; Wesolowski, S. S.; Bunker, P. R.; Dombi, P.; Krausz, F.; Bandrauk, A. D.; Villeneuve, D. M.; Corkum, P. B. Laser Coulomb-explosion imaging of small molecules. *Physical Review A* **2005,** *71* (1), 013415.

31. Atkins, P. W.; De Paula, J. *Atkins' Physical Chemistry*. Macmillan Higher Education: 2006.

32. Frisch, M. J.; Trucks, G. W.; Schlegel, H. B.; Scuseria, G. E.; Robb, M. A.; Cheeseman, J. R.; Scalmani, G.; Barone, V.; Petersson, G. A.; Nakatsuji, H.; Li, X.; Caricato, M.; Marenich, A. V.; Bloino, J.; Janesko, B. G.; Gomperts, R.; Mennucci, B.; Hratchian, H. P.; Ortiz, J. V.; Izmaylov, A. F.; Sonnenberg, J. L.; Williams; Ding, F.; Lipparini, F.; Egidi, F.; Goings, J.; Peng, B.; Petrone, A.; Henderson, T.; Ranasinghe, D.; Zakrzewski, V. G.; Gao, J.; Rega, N.; Zheng, G.; Liang, W.; Hada, M.; Ehara, M.; Toyota, K.; Fukuda, R.; Hasegawa, J.; Ishida, M.; Nakajima, T.; Honda, Y.; Kitao, O.; Nakai, H.; Vreven, T.; Throssell, K.; Montgomery Jr., J. A.; Peralta, J. E.; Ogliaro, F.; Bearpark, M. J.; Heyd, J. J.; Brothers, E. N.; Kudin, K. N.; Staroverov, V. N.; Keith, T. A.; Kobayashi, R.; Normand, J.; Raghavachari, K.; Rendell, A. P.; Burant, J. C.; Iyengar, S. S.; Tomasi, J.; Cossi, M.; Millam, J. M.; Klene, M.; Adamo, C.; Cammi, R.; Ochterski, J. W.; Martin, R. L.; Morokuma, K.; Farkas, O.; Foresman, J. B.; Fox, D. J. *Gaussian 09 Rev. C.01*, Wallingford, CT, 2016.

33. Maté, B.; Tejeda, G.; Montero, S. Raman spectroscopy of supersonic jets of CO2: Density, condensation, and translational, rotational, and vibrational temperatures. *The Journal of Chemical Physics* **1998,** *108* (7), 2676-2685.

34. Ablikim, U.; Bomme, C.; Osipov, T.; Xiong, H.; Obaid, R.; Bilodeau, R. C.; Kling, N. G.; Dumitriu, I.; Augustin, S.; Pathak, S.; Schnorr, K.; Kilcoyne, D.; Berrah, N.; Rolles, D. A coincidence velocity map imaging spectrometer for ions and high-energy electrons to study inner-shell photoionization of gas-phase molecules. *Review of Scientific Instruments* **2019,** *90* (5), 055103.

35. Boo, B. H.; Saito, N.; Suzuki, I. H.; Koyano, I. Dissociation processes of core-excited CBr4 involving the Br(3d, 3p, 3s) and C(1s) inner-shells in the range 50–460 eV. *Journal of Electron Spectroscopy and Related Phenomena* **2002,** *123* (1), 73-84.

36. Chai, J.-D.; Head-Gordon, M. Long-range corrected hybrid density functionals with damped atom–atom dispersion corrections. *Physical Chemistry Chemical Physics* **2008,** *10* (44), 6615-6620.

37. Sreeruttun, R. K.; Ramasami, P. Conformational behaviour of 1,2-dichloroethane and 1,2-dibromoethane: 1H-NMR, IR, refractive index and theoretical studies. *Physics and Chemistry of Liquids* **2006,** *44* (3), 315-328.

38. Tanabe, K. Calculation of infrared band intensities and determination of energy differences of rotational isomers of 1,2-dichloro-, 1,2-dibromo- and 1-chloro-2-bromoethane. *Spectrochimica Acta Part A: Molecular Spectroscopy* **1972,** *28* (3), 407-424.